JOURNAL OF GUIDANCE, CONTROL, AND DYNAMICS
Vol. 27, No. 6, November–December 2004

Design of Reduced-Order Robust Controllers for Smart Structural Systems

Pengxiang Liu* and Vittal S. Rao†
University of Missouri—Rolla, Rolla, Missouri 65401

A method of designing reduced-order robust controllers for smart structural systems, which guarantees the stability and performance of the closed-loop system under various uncertainties, is presented. The uncertainties in structural systems are modeled as norm-bound unstructured uncertainty and structured parametric uncertainties in natural frequencies and damping ratios. Based on the linear matrix inequalities (LMIs) and the Popov criterion, a robust multi-objective controller is designed to suppress the vibrations caused by external disturbances. The limited actuator inputs are also incorporated in the design mythologies. Using LMIs, the order of the synthesized controller is reduced by a frequency-weighted model reduction method. The design procedure was experimentally tested on a multi-input and multi-output three-mass structural test article, which uses piezoelectric actuators and sensors.

Introduction

SMART structure technology[1] enhances structural properties by integrating sensors, actuators, signal processing, and control technologies into structures, resulting in improved disturbance rejection and vibration damping. One example of its applications is the active control of lightly damped spacecraft structure to suppress the vibration caused by external disturbance. For successful integration of the controller with smart structural system, the designed controller has to be a lower-order controller that leads to simple hardware implementation and low power consumption. Because structural systems are vulnerable to various uncertainties, the robustness of the designed controller is essential. The uncertainties in a structural system can be categorized into two classes: norm-bound unstructured uncertainty and parametric uncertainty. Unstructured uncertainty can be caused by neglected high-frequency modes, sensor noise, and actuator gain variation. Parametric uncertainty is caused by the variations of structural parameters around nominal values. The actuators in smart structural systems usually have limited inputs, which affect the performance and the robustness achievable by the control system. These uncertainties and limitations have to be incorporated in the controller design methodologies.

For ensuring unconditional stability to the uncertainties of the structure, most conventional methods[2] for controlling structural systems such as direct velocity feedback, positive position feedback, and positive real synthesis depend on collocated actuator/sensor pairs and some constraints on the controller structure and parameters. The controller parameters are tuned by a trial-and-error procedure in order to satisfy both robust stability and predefined performance simultaneously. This trial-and-error procedure becomes very difficult for multi-input and multi-output (MIMO) structures with a number of controlled modes. Because the robust performance cannot be guaranteed by these methods, the controller parameters have to be modified when the structural parameters are subjected to variations. In addition, the requirement of exact collocation can be restrictive making these methods less attractive for implementation of controllers on generic smart structures. To overcome the restrictions in these conventional methods, we present a robust controller design method for MIMO structures, which does not need the collocation of actuators and sensors, and can simultaneously achieve multiple control objectives: robust performance for uncertainties in structural parameters, robust stability for unmodeled structural dynamics, and a direct consideration of control input constraint in the design.

The proposed design method is based on the linear matrix inequalities (LMIs),[3] which can easily formulate various time and frequency-domain performance constraints and robustness requirements. Because of the recent advances in convex optimization, such as the interior-point algorithm and the availability of user-friendly controller design packages, it has been possible to solve these LMI problems efficiently. The LMI techniques have been applied to the structural control by several researchers. Agrawal et al.[4] have considered the analysis of stability of actively controlled civil engineering structures subject to earthquake vibrations. Niewoehner et al.[5] and Grigoriadis and Skelton[6] have used LMIs on the control of aircraft structures.

In this paper, a structural system with uncertainties is described in modal domain by a linear-fractional-transformation (LFT) model with parametric and unstructured uncertainties. The Popov criterion[7] is used to derive a less conservative condition in terms of LMIs for multi-objective robust controller design. A robust controller is synthesized by solving these LMIs with the help of MATLAB®.[8] The order of the synthesized controller is reduced by a frequency-weighted controller reduction method based on LMIs. Appropriate weighting function is chosen to preserve the system performance in the reduced-order controller. The design method is applied to a three-mass experimental test article, and the experimental results are included.

Representation of Structure with Uncertainty

Throughout this paper, we assume that the structure is a lightly damped flexible structure, and lead-zirconite-tianate (PZT) patches are used as sensors and actuators. The equation of motion of such a structural system can be described in physical coordinates by

$$M\ddot{q}(t) + C_d\dot{q}(t) + K_s q(t) = Fu(t), \qquad y(t) = Lq(t) \quad (1)$$

where $q(t) \in R^{n_m}$ is the vector of structural displacements, M, C_d and K_s are the mass, damping, and stiffness matrices of the structure respectively, input vector $u(t) \in R^l$, and output vector $y(t) \in R^m$.

Following the standard procedure, the structural system can also be represented by a state-space representation in modal coordinates given by

$$\dot{x}_m(t) = A_m x_m(t) + B_m u(t), \qquad y(t) = C_m x_m(t) \quad (2)$$

Received 14 November 2002; revision received 18 October 2003; accepted for publication 7 December 2003.

*Graduate Research Assistant, Department of Electrical and Computer Engineering; Intelligent Systems Center, ERL 305; pliu@umr.edu.

†Professor, Department of Electrical and Computer Engineering; Intelligent Systems Center, ERL 321; raov@umr.edu.

where $A_m = \mathrm{diag}(A_{m1}, \ldots, A_{\mathrm{mi}}, \ldots, A_{\mathrm{mn}_m})$ with

$$A_{\mathrm{mi}} = \begin{bmatrix} -\zeta_i\omega_i & \omega_i\sqrt{1-\zeta_i^2} \\ -\omega_i\sqrt{1-\zeta_i^2} & -\zeta_i\omega_i \end{bmatrix}$$

ζ_i and ω_i are damping ratios and natural frequencies, respectively.

The transfer function of Eq. (2) is given by[9]

$$G_m(s) = \sum_{i=1}^{n_m} L\left[\frac{\psi_i\psi_i^T}{s-\lambda_i} + \frac{\left(\psi_i\psi_i^T\right)^*}{s-\lambda_i^*}\right]F \tag{3}$$

where ψ_i are the complex mode shapes of the structure.

The uncertainties in structural systems can be represented in modal domain as the variations of modal parameters, that is, mode shapes, natural frequencies, and damping ratios. Because natural frequencies and damping ratios determine the structural behavior, the variations in these parameters should be modeled as structured parametric uncertainties. Their variation ranges are determined from measurements or estimations. Because of the difficulty in measuring and modeling the variations of mode shapes having the form of complex vector, their variations can be approximately accounted for by unstructured model uncertainty. Although a flexible smart structure has an infinite number of modes, for simplifying the controller design the structural model Eq. (1) usually represents only the properties of the first n_m modes to be controlled and ignores the dynamics of the structural modes higher than n_m. These neglected high-frequency modes, if not treated properly in controller design, can cause an undesirable spillover effect[10] on the structural system. Hence, to describe the neglected structural modes and the variations in structural parameters, the structure with uncertainty is represented as in Fig. 1.

The matrix Δ_p in Fig. 1 represents the parametric uncertainties in natural frequencies and damping ratios. The stable dynamic system Δ_m with $\|\Delta_m\|_\infty \le 1$ denotes the unstructured uncertainty and is weighted by a high-pass filter function W_m representing the high-frequency uncertainties caused by unmodeled dynamics and the variations in mode shapes. The linear system G in Fig. 1 is derived by performing LFT transformation on Eq. (2) as shown in the following:

Let the uncertain natural frequencies and damping ratios be represented by

$$\omega_i = \omega_{\mathrm{ni}} + \delta_{\omega i}\omega_{\mathrm{ri}} \quad \text{and} \quad \zeta_i = \zeta_{\mathrm{ni}} + \delta_{\zeta i}\zeta_{\mathrm{ri}}, \quad (i = 1, \ldots, n_m) \tag{4}$$

where ω_{ni} and ζ_{ni} denote the nominal values of natural frequency and damping ratio respectively, ω_{ri} and ζ_{ri} define the ranges of their variation around the nominal values, and the uncertain parameters $\delta_{\omega i}$ and $\delta_{\zeta i}$ are normalized as $|\delta_{\omega i}| \le 1$ and $|\delta_{\zeta i}| \le 1$. Then, the A_m matrix of Eq. (2) can be written as $A_m = \mathrm{diag}(A_{m1}, \ldots, A_{\mathrm{mi}}, \ldots, A_{\mathrm{mn}_m})$, where $A_{\mathrm{mi}} \approx (A_{\mathrm{ui}} + \delta_{\omega i}A_{\omega i} + \delta_{\zeta i}A_{\zeta i})$ with

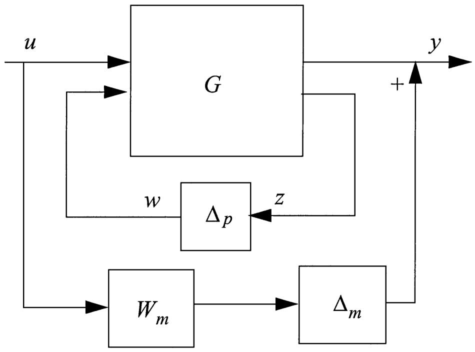

Fig. 1 Representation of structure with uncertainty.

$$A_{\mathrm{ui}} = \begin{bmatrix} -\zeta_{\mathrm{ni}}\omega_{\mathrm{ni}} & \omega_{\mathrm{ni}}\sqrt{1-\zeta_{\mathrm{ni}}^2} \\ -\omega_{\mathrm{ni}}\sqrt{1-\zeta_{\mathrm{ni}}^2} & -\zeta_{\mathrm{ni}}\omega_{\mathrm{ni}} \end{bmatrix}$$

$$A_{\omega i} = \begin{bmatrix} -\zeta_{\mathrm{ni}}\omega_{\mathrm{ri}} & \omega_{\mathrm{ri}}\sqrt{1-\zeta_{\mathrm{ni}}^2} \\ -\omega_{\mathrm{ri}}\sqrt{1-\zeta_{\mathrm{ni}}^2} & -\zeta_{\mathrm{ni}}\omega_{\mathrm{ri}} \end{bmatrix}$$

and

$$A_{\zeta i} = \begin{bmatrix} -\zeta_{\mathrm{ri}}\omega_{\mathrm{ni}} & 0 \\ 0 & -\zeta_{\mathrm{ri}}\omega_{\mathrm{ni}} \end{bmatrix}$$

In the preceding formulation, it is assumed that $1-\zeta_i^2 \approx 1-\zeta_{\mathrm{ni}}^2$ caused by the small damping ratios of lightly damped structure and the second-order uncertain terms $-\delta_{\omega i}\delta_{\zeta i}\zeta_{\mathrm{ri}}\omega_{\mathrm{ri}}$ are neglected.

With the LFT,[11] the system G is given by

$$\dot{x}(t) = Ax(t) + B_m u(t) + B_u w(t), \qquad y(t) = C_m x(t)$$

$$z(t) = C_u x(t), \qquad w(t) = \Delta_p z(t) \tag{5}$$

where the ranges of the uncertain parameters are shifted by the loop transformation to $0 \le \delta_{\omega i}, \delta_{\zeta i} \le 1$ for convenience of controller design,

$$A = \mathrm{diag}\left(A_{u1} - A_{\omega 1} - A_{\zeta 1}, \ldots, A_{\mathrm{un}_m} - A_{\omega n_m} - A_{\zeta n_m}\right)$$

$$\Delta_p = \mathrm{diag}\left(\delta_{\omega 1}I_2, \ldots, \delta_{\omega n_m}I_2, \delta_{\zeta 1}I_2, \ldots, \delta_{\zeta n_m}I_2\right)$$

B_m and C_m are defined in Eq. (2), and B_u, C_u are block diagonal matrices with elements obtained by decomposing $A_{\omega i}$ and $A_{\zeta i}$.

Robust Controller Design

A structure with parametric and unstructured uncertainties, controlled by an output feedback controller, is shown in Fig. 2, where W_f is a low-pass filter function introduced to reduce the spillover effect of the neglected high-frequency modes, K_c is the output feedback controller, w_p and z_p are the disturbance input and performance output, respectively.

The state-space representation of the augmented plant P_a is given by

$$\dot{x}(t) = A_p x(t) + B_p w_p(t) + B_1 w_1(t) + B_2 w_2(t) + Bu(t)$$

$$z_p(t) = C_p x(t) + D_{pp} w_p(t) + E_p u(t), \qquad z_1(t) = C_1 x(t)$$

$$z_2(t) = C_2 x(t) + E_2 u(t), \qquad y(t) = Cx(t) + F_p w_p(t) + F_2 w_2(t)$$

$$w_1(t) = \Delta_p z_1(t) \tag{6}$$

where $A_p \in R^{n\times n}$ and $\Delta_p = \mathrm{diag}(\delta_1 I_2, \ldots, \delta_{n\delta} I_2)$ is a matrix of constant real uncertain parameters δ_i, $i = 1, \ldots, n_\delta$, with $0 \le \delta_i \le 1$.

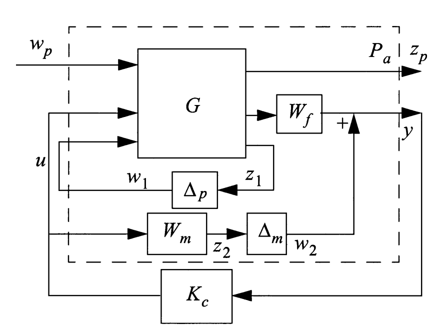

Fig. 2 Representation of closed-loop system with uncertainties.

It is assumed that the controller K_c is strictly proper and has a state-space realization

$$\dot{x}_c(t) = A_c x_c(t) + B_c y(t), \qquad u(t) = C_c x_c(t) \tag{7}$$

Substituting the controller into Eq. (6), the closed-loop system is given by

$$\dot{\bar{x}}(t) = \bar{A}\bar{x}(t) + \bar{B}_p w_p(t) + \bar{B}_1 w_1(t) + \bar{B}_2 w_2(t)$$
$$z_p(t) = \bar{C}_p \bar{x}(t) + D_{pp} w_p(t), \qquad z_1(t) = \bar{C}_1 \bar{x}(t)$$
$$z_2(t) = \bar{C}_2 \bar{x}(t) \tag{8}$$

with

$$\bar{x}(t)^T = \begin{bmatrix} x(t)^T & x_c(t)^T \end{bmatrix}$$

To design a robust controller to suppress the vibration caused by the disturbance input w_p, the following three control objectives are selected:

1) The attenuation of vibration of a structure can be achieved by minimizing the upper bound of the L_2 gain between the disturbance input w_p and performance output z_p:

$$\min\left\{\gamma : \int_0^\infty \|z_p\|^2 \,\mathrm{d}t < \gamma^2 \int_0^\infty \|w_p\|^2 \,\mathrm{d}t\right\} \tag{9}$$

This performance should be robust for parametric uncertainties represented by Δ_p.

2) The closed-loop system should be stable under the neglected structural dynamics and other uncertainties, represented by Δ_m in Fig. 2. From the small-gain theorem,[11] the stability is guaranteed if the L_2 gain between w_2 and z_2 is less than one, that is,

$$\int_0^\infty \|z_2\|^2 \,\mathrm{d}t < \int_0^\infty \|w_2\|^2 \,\mathrm{d}t \tag{10}$$

3) The limited actuator input is directly considered in the controller design by forcing the controller outputs within the input limits of actuators when the disturbance input w_p is bounded by a finite energy E_m, that is,

$$|u_i(t)| \le u_{\max} \qquad \text{s.t.} \int_0^\infty w_p^T w_p \,\mathrm{d}t \le E_m \qquad \text{for} \qquad i = 1, \ldots, l \tag{11}$$

where l is the number of controller outputs. For simplicity, only the nominal closed-loop system, that is, a system with $\Delta_m = 0$ and $\Delta_p = 0$, needs to satisfy Eq. (11). Note that there is a tradeoff between the system performance γ and the disturbance energy E_m: setting up a smaller E_m leads to a higher-gain controller having better performance, but its outputs are more susceptible to saturating actuators.

By the bounded real lemma[3] and the Popov criterion, a closed-loop system with the parametric uncertainties as shown in Fig. 2 is known to have robust L_2 gain bounded by γ if there exists a positive definite matrix $P(\Delta_p) = P_1 + \bar{C}_1^T \Lambda \, \Delta_p \, \bar{C}_1$ such that[12]

$$\begin{bmatrix} \bar{A}(\Delta_p)^T P(\Delta_p) + P(\Delta_p)\bar{A}(\Delta_p) & P(\Delta_p)\bar{B}_p & \bar{C}_p^T \\ \bar{B}_p^T P(\Delta_p) & -I & D_{pp}^T \\ \bar{C}_p & D_{pp} & -\gamma^2 I \end{bmatrix} < 0 \tag{12}$$

where $\bar{A}(\Delta_p) = \bar{A} + \bar{B}_1 \Delta_p \bar{C}_1$ and Λ is a symmetric block diagonal matrix in the form $\Lambda = \mathrm{diag}(\Lambda_1, \ldots, \Lambda_i, \ldots \Lambda_{n\delta})$ with $\Lambda_i \in R^{2\times 2}$.

Because the uncertain parameters δ_i are bounded by $0 \le \delta_i \le 1$, the block diagonal matrix Δ_p satisfies the following matrix inequality:

$$\begin{bmatrix} \Delta_p \\ I \end{bmatrix}^T \begin{bmatrix} -(R + R^T) & R \\ R^T & 0 \end{bmatrix} \begin{bmatrix} \Delta_p \\ I \end{bmatrix} \ge 0 \qquad \text{with} \qquad R + R^T > 0 \tag{13}$$

where $R = \mathrm{diag}(R_1, \ldots, R_i, \ldots R_{n\delta})$ with $R_i \in R^{2\times 2}$.

Based on Eq. (13), it can be proven by using the S procedure[3] that Eq. (12) is satisfied if there exists a positive definite matrix $P_1 = P_1^T > 0$ such that

$$\begin{bmatrix} \bar{A}^T P_1 + P_1 \bar{A} & (\ldots)^T & (\ldots)^T & \bar{C}_p^T \\ \bar{B}_p^T P_1 & -I & (\ldots)^T & D_{pp}^T \\ \bar{B}_1^T P_1 + \Lambda \bar{C}_1 \bar{A} + R\bar{C}_1 & \Lambda \bar{C}_1 \bar{B}_p & He(\Lambda \bar{C}_1 \bar{B}_1 - R) & 0 \\ \bar{C}_p & D_{pp} & 0 & -\gamma^2 I \end{bmatrix} < 0 \tag{14}$$

where $He(\Theta) := \Theta + \Theta^T$.

By the bounded real lemma, the second objective regarding the stability under the unstructured uncertainty Δ_m is satisfied if there exists a positive definite matrix P_2 such that

$$\begin{bmatrix} \bar{A}^T P_2 + P_2 \bar{A} & P_2 \bar{B}_2 & \bar{C}_2^T \\ \bar{B}_2^T P_2 & -I & 0 \\ \bar{C}_2 & 0 & -I \end{bmatrix} < 0 \tag{15}$$

To find a controller that can satisfy both Eqs. (14) and (15), we let $P_1 = P_2 = P$. This arbitrary equalization of two different matrices makes the design of multi-objective controller feasible. However, this controller becomes conservative.

The relationship between system state and disturbance input defined by Eq. (14) yields

$$\bar{x}_n(t)^T P \bar{x}_n(t) < \int_0^t w_p(\tau)^T w_p(\tau) \,\mathrm{d}\tau$$

where $\bar{x}_n(t)$ denotes the state of the nominal closed-loop system. When the system is driven by the energy-bounded disturbance input w_p, the system states belong to a set defined by $\{\bar{x}_n(t) : \bar{x}_n(t)' P \bar{x}_n(t) < E_m\}$; hence, the controller outputs vary in a range[3] bounded by $u_{\max}$ if

$$E_m \begin{bmatrix} 0 \\ C_{ci}^T \end{bmatrix} [0 \quad C_{ci}] < u_{\max}^2 P, \qquad i = 1, \ldots, l \tag{16}$$

is satisfied, where C_{ci} is the ith output vector of the controller.

The matrix inequalities Eqs. (14) and (15) are not convex in the controller parameters and matrix P. But they can be transformed to convex ones by using a standard LMI controller synthesis procedure.[13] Let

$$P = \begin{bmatrix} X & U \\ U^T & * \end{bmatrix}$$

and

$$P^{-1} = \begin{bmatrix} Y & V \\ V^T & * \end{bmatrix}$$

By introducing new variables K, L, and M, Eqs. (14–16) can be transformed respectively to the following equivalent matrix inequalities, which are convex in matrices X, Y, K, L, and M:

$$\begin{bmatrix} He(A_pY+BM) & (\ldots)^T & B_p & Q^T & (\ldots)^T \\ A_p^T+K & He(XA_p+LC) & (\ldots)^T & (\ldots)^T & C_p^T \\ B_p^T & B_p^TX+F_p^TL^T & -I & (\ldots)^T & D_{\mathrm{pp}}^T \\ Q & B_1^TX+\Lambda C_1A_p+RC_1 & \Lambda C_1B_p & He(\Lambda C_1B_1-R) & 0 \\ C_pY+E_pM & C_p & D_{\mathrm{pp}} & 0 & -\gamma^2 \end{bmatrix} < 0 \tag{17}$$

$$\begin{bmatrix} He(A_pY+BM) & (\ldots)^T & B_2 & (\ldots)^T \\ A_p^T+K & He(XA_p+LC) & (\ldots)^T & C_2^T \\ B_2^T & B_2^TX+F_2^TL^T & -I & 0 \\ C_2Y+E_2M & C_2 & 0 & -I \end{bmatrix} < 0 \quad \text{and} \quad \begin{bmatrix} Y & I & M_i^T \\ I & X & 0 \\ M_i & 0 & u_{\max}^2/E_m \end{bmatrix} > 0 \tag{18}$$

where $Q=B_1^T+\Lambda C_1(A_pY+BM)+RC_1Y$, M_i for $i=1,\ldots,l$ are the ith row of matrix M.

The controller parameters are constructed by

$$\begin{bmatrix} A_c & B_c \\ C_c & 0 \end{bmatrix} = \begin{bmatrix} U & XB \\ 0 & I \end{bmatrix}^{-1} \begin{bmatrix} K-XA_pY & L \\ M & 0 \end{bmatrix} \begin{bmatrix} V^T & 0 \\ CY & I \end{bmatrix}^{-1} \tag{19}$$

where $UV^T=I-XY$.

Synthesizing a robust controller satisfying the preceding three control objectives is then formulated as solving the optimization problem:

$$\min \gamma \text{ s.t. Eqs.(17) and (18)} \tag{20}$$

where the decision variables are matrices K, L, and M, positive definite matrices X and Y, and multipliers Λ and R. Equation (20) is not a convex problem with respect to these variables unless the multipliers R and Λ are already known. Therefore, the following iterative steps are applied to designing a robust controller for structural systems with parametric and unstructured uncertainties.

1) Step 1: Initialize the controller parameters by finding a controller for the nominal system with no parametric uncertainty.

2) Step 2: With the controller parameters fixed, search for matrices P, R, and Λ to minimize the performance γ subject to Eqs. (14–16).

3) Step 3: By using the matrices R and Λ calculated from the preceding step, solve Eq. (20) and determine the robust controller by Eq. (19).

4) Step 4: Iteratively apply steps 2 and 3 until the performance γ converges.

The controller synthesized by this approach is conservative as a result of several factors. First, all of the constraints for the multiobjective design are based on a single Lyapunov function, which only formulates a sufficient condition for a controller satisfying both robustness and performance. Second, because these constraints are solved by an iterative scheme compromising of analysis and synthesis steps the resulting controller is not the optimal solution. Third, the time-invariant nature of the real parametric uncertainty cannot be fully captured by the Popov criterion although it is less conservative than the circle criterion and μ-synthesis condition. The conservatism is also attributed by the way that the parametric uncertainties of structures are modeled as individual variations, which form a set of variations much larger than the actual physical variations.

Besides the conservatism of this approach, another concern is its numerical difficulty, which increases with the number of the controlled modes n_m and the uncertain parameters n_δ. The numbers of decision variables in the analysis step (step 2) and synthesis step (step 3) are $n(2n+1)+7n_\delta$ and $n(n+1)+n^2+(m+l)n$, respectively, where $n=2n_m+n_w$, and n_w denotes the sum of the orders of weighting functions in Fig. 2. Because the interior-point LMI algorithm has polynomial-time complexity with respect to the number of decision variables, the iterative scheme might have numerical difficulties for large-scale structures.

Controller Reduction

The robust controller synthesized by the preceding scheme has an order equal to the order of structural model G plus the orders of weighting functions W_f and W_m. Because simple hardware implementation of the controller is critical to smart structure systems, this higher-order controller needs to be reduced to a lower-order one for a desired performance. The following LMI-based controller reduction method is presented to achieve this goal.

The reduced-order controller $K_r(s)$ is modeled as the full-order controller $K_c(s)$ with additional error[14] $\Delta_r(s)$ frequency-weighted by $W(s)$, that is, $K_r(s)=K_c(s)-\Delta_r(s)W(s)$. Note that there should be no direct term in the reduced-order controller in order to avoid the spillover effect of unmodeled high-frequency modes. To preserve the performance in the reduced-order controller, the weighting function $W(s)$ should be appropriately chosen, and the controller reduction error should be smaller in terms of its H_∞ norm

$$E=\|\Delta_r(s)\|_\infty=\left\|[K_c(s)-K_r(s)]W(s)^{-1}\right\|_\infty$$

From the control objective two, we have $\|W_mK_c(I-W_fGK_c)^{-1}\|_\infty<1$ that leads to

$$\bar\sigma[K_c(j\omega)]<\bar\sigma[I-W_f(j\omega)G(j\omega)K_c(j\omega)]\bar\sigma\left[W_m^{-1}(j\omega)\right] \quad \text{for all} \quad \omega\in R \tag{21}$$

where the symbol $\bar\sigma(V)$ denotes the largest singular value of matrix V. Because $W_m(s)$ is a high-pass filter and $\bar\sigma[I-W_f(j\omega)G(j\omega)K_c(j\omega)]$ has larger values in the low-frequency band, Eq. (21) shows that the spectrum energy of the full-order controller $K_c(s)$ concentrates on the low-frequency band, which primarily determines the controller performance. Therefore, the weighting function $W(s)$ should be chosen as a high-pass filter, allowing good approximation of the performance-sensitive low-frequency band and larger reduction error in the high-frequency band having little effect on the performance.

The commonly used frequency-weighted model reduction methods are the extensions of the balanced truncation and the optimal Hankel norm reduction methods. The reduced-order controllers generated by these methods usually have larger reduction errors, which can be reduced by the following LMI-based method.

Suppose the frequency-weighted error model $[K_c(s)-K_r(s)]W(s)^{-1}$ has a state-space realization

$$\begin{bmatrix} \dot x_k(t) \\ \dot x_r(t) \\ z(t) \end{bmatrix} = \begin{bmatrix} A_k & 0 \\ B_rC_k & A_r \\ C_{\mathrm{kk}} & -C_r \end{bmatrix} \begin{bmatrix} x_k(t) \\ x_r(t) \end{bmatrix} + \begin{bmatrix} B_k \\ B_rD_w \\ 0 \end{bmatrix} w(t) \tag{22}$$

where

$$A_k = \begin{bmatrix} A_c & B_c C_w \\ 0 & A_w \end{bmatrix}, \qquad B_k = \begin{bmatrix} B_c D_w \\ B_w \end{bmatrix}$$

$$\begin{bmatrix} C_k \\ C_{\text{kk}} \end{bmatrix} = \begin{bmatrix} 0_{m\times n} & C_w \\ C_c & 0_{l\times \text{nw}} \end{bmatrix}, \qquad \begin{bmatrix} A_w & B_w \\ C_w & D_w \end{bmatrix}$$

$$\text{and} \qquad \begin{bmatrix} A_r & B_r \\ C_r & 0 \end{bmatrix}$$

are the state-space realizations of $W(s)^{-1}$ and $K_r(s)$ respectively, $A_c \in R^{n\times n}$, $A_w \in R^{nw\times nw}$, and $A_r \in R^{nr\times nr}$ with $nr < n$.

From the bounded real lemma, we have $E < \gamma_e$ if and only if there exists a positive definite matrix P_r such that

$$\begin{bmatrix} He\left(\begin{bmatrix} A_k & 0 \\ B_r C_k & A_r \end{bmatrix}^T \begin{bmatrix} P_{r1} & P_{r3} \\ P_{r3}^T & P_{r2} \end{bmatrix}\right) & (\ldots)^T & (\ldots)^T \\ \left[B_k^T D_w^T B_r^T\right] \begin{bmatrix} P_{r1} & P_{r3} \\ P_{r3}^T & P_{r2} \end{bmatrix} & -\gamma_e I & 0 \\ [C_{\text{kk}} \quad -C_r] & 0 & -\gamma_e I \end{bmatrix} < 0$$

where

$$\begin{bmatrix} P_{r1} & P_{r3} \\ P_{r3}^T & P_{r2} \end{bmatrix} = P_r \tag{23}$$

Because Eq. (23) is a bilinear matrix inequality with respect to the unknown reduced-order controller and the matrix P_r, it cannot be solved by LMI techniques. But if the element P_{r3} of the matrix P_r has a special form

$$P_{r3} = \begin{bmatrix} P_{r4} \\ 0 \end{bmatrix} \in R^{(n+nw)\times nr} \tag{24}$$

where $P_{r4} \in R^{nr\times nr}$ is a nonsingular square matrix, the bilinear matrix inequality is equivalent to a linear matrix inequality as follows:

There exist matrices P_{r1}, P_{r0} and

$$\begin{bmatrix} A_f & B_f \\ C_f & 0 \end{bmatrix}$$

such that

$$P_{r1} - \begin{bmatrix} P_{r0} & 0 \\ 0 & 0 \end{bmatrix} > 0$$

$P_{r0} > 0$ and

$$\begin{bmatrix} He\left(A_k^T P_{r1} + S B_f C_k\right) & (\ldots)^T & (\ldots)^T & (\ldots)^T \\ A_f^T S^T + P_{r0} S^T A_k + B_f C_k & A_f^T + A_f & (\ldots)^T & -C_f^T \\ B_k^T P_{r1} + D_w^T B_f^T S^T & B_k^T S P_{r0} + D_w^T B_f^T & -\gamma_e I & 0 \\ C_{\text{kk}} & -C_f & 0 & -\gamma_e I \end{bmatrix} < 0 \tag{25}$$

where

$$S = \begin{bmatrix} I_{\text{nr}} \\ 0 \end{bmatrix}$$

$P_{r0} \in R^{nr\times nr}$. A reduced-order controller is then given by

$$\begin{bmatrix} A_r & B_r \\ C_r & 0 \end{bmatrix} = \begin{bmatrix} P_{r4}^{-1} & 0 \\ 0 & I \end{bmatrix} \begin{bmatrix} A_f & B_f \\ C_f & 0 \end{bmatrix} \begin{bmatrix} \left(P_{r4}^{-1}\right)^T P_{r2} & 0 \\ 0 & I \end{bmatrix}$$

$$\text{with} \qquad P_{r0} = P_{r4} P_{r2}^{-1} P_{r4}^T \tag{26}$$

Equation (25) is derived by postmultiplying and premultiplying Eq. (23) with $J = \text{diag}(I_{n+\text{nw}}, P_{r2}^{-1} P_{r4}^T, I_m, I_l)$ and its transpose, respectively.

The general form of P_{r3} can be represented as

$$P_{r3} = \begin{bmatrix} P_{r4} \\ N P_{r4} \end{bmatrix}$$

with $P_{r4} \in R^{nr\times nr}$ being nonsingular and $N \in R^{(n+nw-nr)\times nr}$. Then, P_{r3} in Eq. (23) can be transformed to the special form Eq. (24) by premultiplying and postmultiplying Eq. (23) with $T_r = \text{diag}(L_r, I_{\text{nr}}, I_m, I_l)$ and its transpose, respectively, where

$$L_r = \begin{bmatrix} I_{\text{nr}} & 0 \\ -N & I_{n+\text{nw}-\text{nr}} \end{bmatrix}$$

Similar to the controller design, the controller reduction error can be iteratively reduced by getting the matrix N from Eq. (23) with fixed A_r and B_r and then obtaining the reduced-order controller from the solution of Eq. (25). The reduction error will not converge to its minimal with this iterative scheme. The iterative scheme can start with a reduced-order controller from any controller reduction method, and thus the final resulting reduction error relies closely on the initialization. The application of the proposed method is limited to stable controllers for it is derived from a Lyapunov function. Because it cannot be ensured that a reduced-order controller having smaller reduction error preserves the performance and the robustness of the full-order controller, posterior system analysis is thus indispensable for determining whether it satisfies the control requirements for the closed-loop system.

Experimental Results

For experimental verification of the robust controller design and controller reduction methods just presented, a three-mass smart structure test article as shown in Fig. 3 was used.

This structure consists of three wooden blocks connected by two strips of aluminum and is mounted on a steel frame in a pendulum configuration, where the top of the structure is clamped to the frame and the bottom is left to hang free as shown in Fig. 3. The PZT patches are mounted on the structure for actuation and sensing purposes, and their placement locations are chosen to achieve effective control of the vibrations of the first three modes. It can be noticed that the actuators and sensors are not collocated in the experiment. The PZT sensors have low noise and high-frequency bandwidth. The control computer consists of the dSPACE system, which builds a discreate realization of the synthesized continuous controller directly from Simulink using Euler numerical integration method with

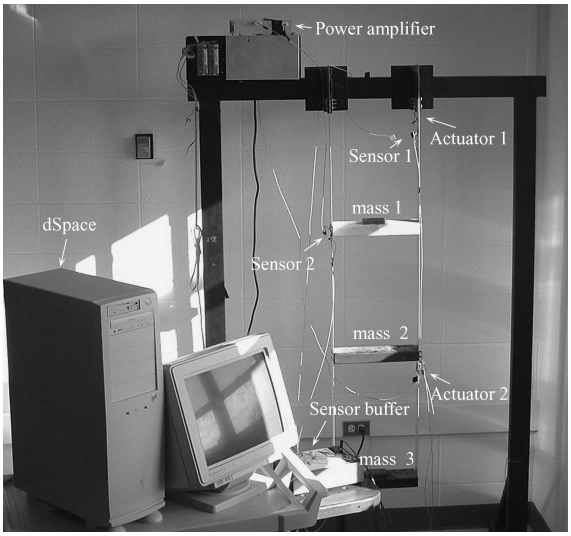

Fig. 3 Three-mass structure experimental setup.

a sampling frequency of 5 kHz. In this experiment, the discretization effect can almost be ignored because of this high sampling rate. The outputs from the control computer are amplified by power amplifiers of gain 30, whose outputs, limited between ±150 volts, drive the actuators. This translates into a limitation of 5 V at the input of the PZT driver power amplifier, which has a 1-KHz bandwidth and can provide a maximum 9-W power. The signals from PZT sensors, measuring the structural displacement in voltage, are fed back to the controller after passing through a high-resistance buffer circuit. With swept-sine frequency response measurements and curve fitting, a sixth-order state space model of two inputs and two outputs is obtained for describing the first three modes of the structure with the natural frequencies 1.76, 4.49, and 6.86 Hz, and damping ratios 0.0062, 0.009, and 0.0047. The natural frequencies and damping ratios of the first three modes are assumed to have ±10% variation ranges around their nominal values. To reduce the spillover effect, a low-pass filter $W_f(s)$ is chosen to be

$$W_f(s) = [150/(s+150)]I_2$$

The following control objectives are selected for a desired performance and robustness:

1) The L_2 gain between actuator 2 and sensor 1 should be minimized when the structural parameters vary within the defined ranges.

2) The closed-loop system should be stable under the additive model uncertainty represented by norm-bound uncertainty weighted by the function

$$W_m(s) = \frac{s+150}{10(s+300)}\begin{bmatrix}\dfrac{s+150}{s+300} & 0\\ 0 & 1\end{bmatrix}$$

3) To consider the actuator saturation in the design, the controller outputs are limited between −5 and 5 V when the disturbance has energy less than 0.143.

Using the iterative scheme, an 11th-order controller satisfying the preceding objectives is synthesized. The system performance converges to (−13.56 dB) from an initial value (−8.4 dB) in four iterations. The synthesized 11th-order controller is then reduced by the frequency-weighted model reduction method with the weighting function chosen to be

$$W(s) = \frac{(s+1)(s+200)}{100}\begin{bmatrix}1 & 0\\ 0 & 1.25\end{bmatrix}$$

In Fig. 4, the LMI-based reduction method is compared with the commonly used frequency-weighted balanced truncation method. Figure 4 shows the reduced-order controller by the LMI-based method has smaller reduction error. It also shows a large increase of reduction error at the fifth order controller. Posterior performance analysis indicates that the sixth-order controller has a robust performance of (−14.57 dB), very close to the (−14.62 dB) of the full-order controller, but the performance of the fifth-order controller deteriorates to (−11.4 dB). Therefore, the sixth-order controller preserving the performance is chosen for further analysis and experimental tests.

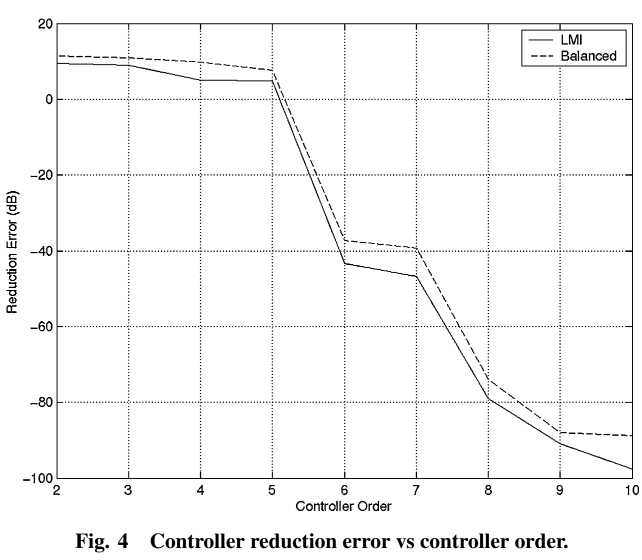

Fig. 4 Controller reduction error vs controller order.

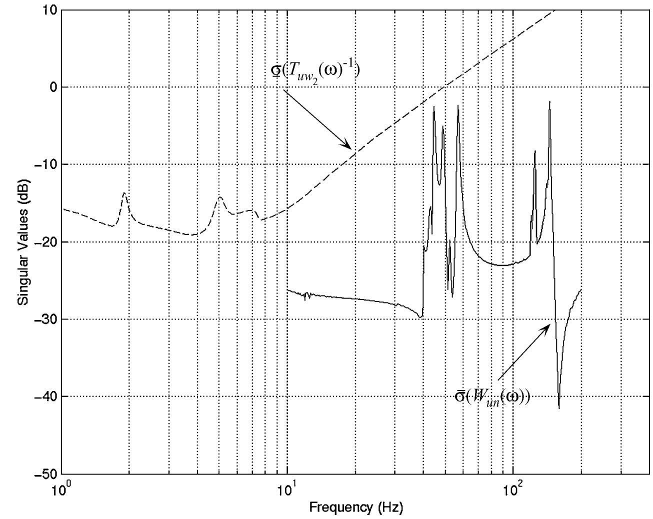

Fig. 5 Robust stability analysis.

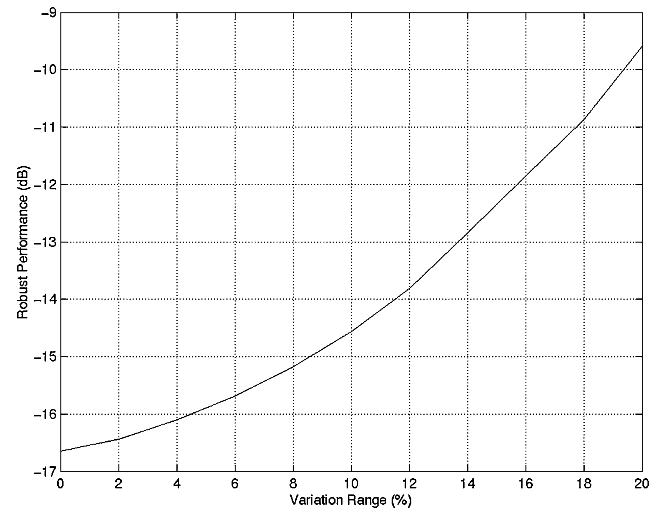

Fig. 6 Performance vs the parametric uncertainty.

Using the small-gain theorem, the robust stability of the closed-loop system for unmodeled dynamics is verified in Fig. 5 by showing

$$\bar{\sigma}[W_{\mathrm{un}}(\omega)] < \underline{\sigma}\left[T_{\mathrm{uw}_2}(\omega)^{-1}\right] \qquad \text{for all} \qquad \omega \in R$$

in the unmodeled frequency region 10 Hz $\leq \omega \leq$ 200 Hz, where $\bar{\sigma}$ and $\underline{\sigma}$ are the maximum and minimum singular values, respectively; $W_{\mathrm{un}}(\omega)$ is the experimentally measured frequency response of the unmodeled structural dynamics; and $T_{\mathrm{uw}_2}(\omega)$ denotes the frequency response of the closed-loop system between the output w_2 and the input u.

The robustness of this sixth-order controller for parametric uncertainties is shown in Fig. 6. The performance deteriorates less than 2 dB for a 10% variation in structural parameters.

Using dSPACE system, the sixth-order controller was implemented to control the three-mass structure. In addition to the nominal structure, two test cases are set up by reducing or adding the weights of mass 1 and mass 3 to simulate the variations in structural parameters as shown in Table 1, where the symbols f and d denote natural frequency and damping ratio, respectively.

The controller significantly improves the disturbance rejection property of the structure from 1.5 dB to (−16.5 dB) as shown in

Table 1 Variations of structural parameters in two test cases

	First mode		Second mode		Third mode	
Weights	f,%	d,%	f,%	d,%	f,%	d,%
Reducing	7.9	5.7	9.9	−5.6	6.8	6.4
Adding	6.9	8.1	7.4	−8.8	4.1	−4.2

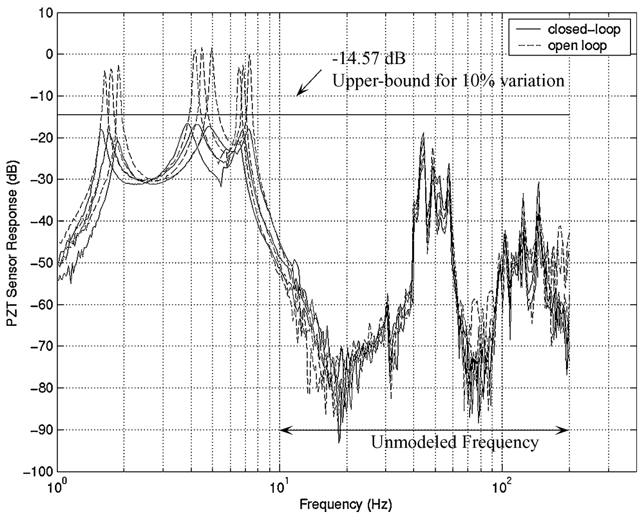

Fig. 7 Frequency responses of closed-loop and open-loop systems.

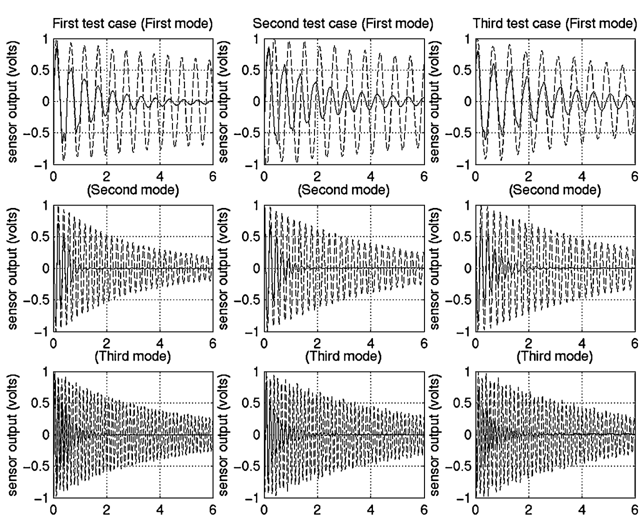

Fig. 8 Damping responses in three modes (– – –, open loop; ——, closed loop).

Fig. 7. The experimentally tested frequency responses in Fig. 7 confirms the robust performance of the designed controller: the L_2 gains of the closed-loop systems are bounded by (−14.57 dB) as shown in Fig. 6 for a 10% variation range. Showing the frequency responses of the closed-loop and open-loop systems in unmodeled high-frequency band, Fig. 7 also verifies experimentally that the controller retains robust stability as indicated by Fig. 5. For comparison, we also tested the performance of a controller designed without considering any uncertainty of the structure. The variations in structural parameters cause the closed-loop systems unstable.

Figure 8 shows the damping responses of the first three modes in the three test cases. It is clear that when active control is applied the vibrations decay much faster than in open-loop systems. Because the decay rates of the closed-loop systems in the three test cases change little, the robustness of the controller is also verified by these time responses.

Conclusions

We investigated the reduced-order robust controller design for smart structural systems with model uncertainties and limited actuator inputs. By introducing unstructured uncertainty and parametric uncertainties in natural frequencies and damping ratios, it is shown in the design of robust controller that the controller can achieve the robustness and performance. With smaller reduction error, the synthesized high-order controller is reduced by a LMI-based frequency-weighted controller reduction method. The presented methods were successfully tested on a three-mass structure of two inputs and two outputs.

There are several conservative factors in the proposed approaches: the modeling of uncertain parameters, the formulation of multi-objective design problem, and the solution to nonconvex matrix inequalities. The LMI-based methods also suffer numerical difficulty in their applications to large-scale structures. Further research is needed to solve these problems.

References

[1]Srinivasan, A. V., and McFarland, D. M., *Smart Structures: Analysis and Design*, Cambridge Univ. Press, New York, 2001, pp. 1–6.

[2]Preumont, A., *Vibration Control of Active Structures*, 2nd ed., Kluwer Academic, Norwell, MA, 2002, pp. 91–102.

[3]Boyd, S., Ghaoui, L. E., Feron, E., and Balakrishnan, V., *Linear Matrix Inequalities in System and Control Theory*, Studies in Applied Mathematics, Vol. 15, Society of Industrial and Applied Mathematics, Philadelphia, 1994, pp. 23, 24, 26, 27, and 77–81.

[4]Agrawal, A. K., Yang, J. N., Schimtendorf, W. E., and Jabbari, F., "Stability of Actively Controlled Structures with Actuator Saturation," *Journal Structural Engineering*, Vol. 123, No. 4, 1997, pp. 505–512.

[5]Niewoehner, R. J., and Kaminer, I. I., "Integrated Aircraft-Controller Design Using Linear Matrix Inequalities," *Journal of Guidance, Control, and Dynamics*, Vol. 19, No. 2, 1996, pp. 445–452.

[6]Grigoriadis, K. M., and Skelton, R. E., "Integrated Structural and Control Design for Vector Second-Order Systems via LMIs," *Proceedings of the American Control Conference*, Vol. 3, American Automatic Control Council, Evanston, IL, 1998, pp. 1625–1629.

[7]Khalil, H. K., *Nonlinear Systems*, 3rd ed., Prentice–Hall, Upper Saddle River, NJ, 2002, pp. 275–279.

[8]Gahinet, P., Nimirovski, A., and Laub, A. J., *LMI Control Toolbox: User's Guide*, The MathWorks, Inc., Natick, MA, 1995.

[9]Lee, C. G., and Yun, C. B., "Parameter Identification of Linear Structural Dynamic Systems," *Journal of Computers and Structures*, Vol. 40, No. 6, 1991, pp. 1475–1487.

[10]Balas, M. J., "Trends in Large Space Structures Control Theory: Fondest Hopes, Wildest Dreams," *IEEE Transactions on Automatic Control*, Vol. 27, No. 6, 1982, pp. 522–535.

[11]Zhou, K., and Doyle, J. C., *Robust and Optimal Control*, Prentice–Hall, Upper Saddle River, NJ, 1996, pp. 247–269, 217–221.

[12]Feron, E., Apkarian, P., and Gahinet, P., "Analysis and Synthesis of Robust Control Systems via Parameter-Dependent Lyapunov Functions," *IEEE Transactions on Automatic Control*, Vol. 41, No. 7, 1996, pp. 1041–1046.

[13]Scherer, C., and Weiland, S., *Lecture Notes DISC Course on Linear Matrix Inequalities in Control*, Ver. 2.0, April 1999, pp. 65–82.

[14]Goddard, P. J., and Glover, K., "Controller Approximation Approaches for Preserving H_∞ Performance," *IEEE Transactions on Automatic Control*, Vol. 43, No. 7, 1998, pp. 858–870.